Lab on a Chip

Accepted Manuscript

ROYAL SOCIETY
OF CHEMISTRY

www.rsc.org/loc

Journal Name RSCPublishing

ARTICLE

Cyclic Olefin Copolymer Plasma Millireactors

G. Schelcher[a], C. Guyon[a], S. Ognier[a,b], S. Cavadias[a,b], E. Martinez[a], V. Taniga[c], L. Malaquin[c], P. Tabeling[d] and M. Tatoulian[a]

……………………………………………
……………………………………+x

Cite this: DOI: 10.1039/x0xx00000x

Received 00th January 2012,
Accepted 00th January 2012

DOI: 10.1039/x0xx00000

www.rsc.org/

The novelty of this paper lies in the development of a multistep process for the manufacturing of plasma millireactors operating at atmospheric pressure. The fabrication process relies on the integration of metallic electrodes over a Cyclic Olefin Copolymer chip by a combination of photopatterning and sputtering. The developed plasma millireactors were successfully tested by creating air discharges in the gas volume of the millichannel. A sputtered silica layer was deposited on the channel walls to provide a barrier between the plasma and the polymer in order to prevent the alteration of polymer surfaces during the plasma treatment. The interest of this process for employing plasma millireactor as high reactive environment is demonstrated here by the case of degradation of a Volatile Organic Compound (acetaldehyde) in ambient air. In this miniaturized device, we obtained a high acetaldehyde conversion (98 %) for a specific input energy lower than 200 J.L^{-1}.

Introduction

Nowadays, non-thermal discharges at atmospheric pressure are of great interest to many fields owing to the highly reactive environment provided at relatively cold temperatures. Moreover, plasma processes are known to be environmentally friendly and an energy saving processing route [1]. Miniaturization of plasma reactors has the promise of producing the plasma at much lower voltages than conventional scale reactor, and thus achieving low power production. In addition, the microscale dimensions reduce the transport of both heat and mass, and so provide a nearly isothermal, rapid-mixing homogeneous environment for efficient chemical reactions. Thus, generation of plasmas in micro and millichannels may lead to a better control of chemical transformations.

Plasmas reactors used as a milli-scale source of ions, excited species and radicals open several opportunities for the chemical process intensification and could be an enabling technology across fundamental and applied science. Indeed, these microplasmas can be generated at relatively low gas temperatures and possess an electron energy distribution containing large fractions of high-energy electrons which lead to the production of reactive species [2].

Thus, the implementation of atmospheric plasma into sub-mm volume has become increasingly attractive for the efficient synthesis of valuable chemicals and nanostructures as well as for the decomposition of hazardous compounds [3,4].

These miniaturized plasma reactors can be classified based on the application, the electric field switching frequency ranging from DC to GHz, the geometries extending from dielectric barrier discharges [5] to micro hollow cathodes [6] and microcavity discharges [7]. Several studies have shown the interest of using plasma microreactors for environmental applications (such as the conversion of Volatile Organic Compounds [4,8,9], the conversion and activation of alkanes [10,11]), for the synthesis of nanoparticles [12,13], as UV radiation sources and also as plasma cathodes [14]. An overview of their applications can be found in some interesting review papers [4,14,15].

The Dielectric Barrier Discharge (DBD) configuration is one of the most advantageous approaches to favor the reliability of the plasma chip. In this configuration, a dielectric layer separates the electrodes from the plasma region. This layer acts as an insulator and so prevents spark formation which can potentially cause device failure during plasma treatments. In this case, the plasma has a capacitive nature and consists of a large number of filamentary microdischarges within the gas gap. The duration of these microdischarges is limited to a few nanoseconds. Thus, gas heating is minimized, whereas the activation of molecules and atoms in the gas volume is ensured by the large fractions of high-energy electrons [16].

Dielectric barriers can be made of various insulating materials like glass, ceramic or polymer coatings [17,18]. Hard materials, such as glass or silicon, are commonly employed for the fabrication of plasma millireactors [13,19]. This is due to their ability in achieving small feature patterns. These materials also exhibit a good solvent compatibility and provide a suitable surface stability. Glass, in particular, is considered as the material of choice due to its electrical insulating properties and beneficial optical transparency which allows in-situ diagnostics such as optical emission spectroscopy or ultra-rapid camera measurement. However, the rapid prototyping of hard materials is severely limited due to the need for cleanroom facilities, the high cost involved in processing and the cost of the material itself [20]. Additionally, glass micromachining processes are technically demanding and time consuming. To overcome these drawbacks, polymers offer an attractive alternative to hard materials for rapid prototyping of miniaturized plasma reactor. They are relatively inexpensive, adaptable through formulation changes or chemical modification [21], and generally have faster fabrication processes (e.g., hot embossing, injection molding, etc.) [22]. Moreover, most of the polymers used in microfabrication exhibit a glass like transparency. Some authors do use polymers like ultraviolet-curable polymer [23] or Teflon® [5] as spacer for the fabrication of plasma millireactors. However, even in those cases, hard materials such as glass are still involved.

Experimental

Principle

In this paper, we propose to elaborate on and investigate a DBD polymer miniaturized plasma system aimed at the volatile organic compound (VOC) elimination in ambient air.

We chose COC (Cyclic Olefin Copolymer) as a base material for the fabrication of the proposed DBD millireactor. COC is a thermoplastic copolymer composed of norbornene and ethylene groups. Its properties directly depends on the norbornene-to-ethylene ratio such as its glass transition temperature (T_g) which ranges from 70 °C up to 180 °C. Other polymeric materials such as polydimethylsiloxane, polymethyl methacrylate, or polystyrene could likely be used as the microreactor material but the COC has the advantage of being easily shaped, exhibiting good electrical insulating properties (Dielectric constant is 2.35 at 60 Hz) and it can be easily coated using conventional vacuum techniques without any surface processing [24,25]. These characteristics are well suited for the realization of a plasma millireactor operating under cold plasma conditions while its glass like transparency [26] is helpful to perform in-situ diagnostics of the discharge (Optical Emission Spectroscopy (OES) or Ultra-rapid camera measurements). Furthermore, COC is resistant to hydrolysis, acids, alkalis, as well as polar solvents. Thus, this material can withstand several technological steps including photo-patterning development, wet etching and surface functionalization stable upon aging [25]. Owing to these properties, the COC is a great candidate for a plasma millireactor material. Moreover, submicron-size surface features could be easily reproduced using conventional molding techniques due to the good flow ability of this polymer [27].

Figure 1 shows the main technological steps: the COC cap formation by molding (Figure 1.a), the electrode elaboration by a combination of photopatterning and sputtering (Figure 1.b), the passivation of the channel inner surfaces (Figure 1.b), the alignment and finally the thermal fusion bonding of the chip (Figure 1.c).

The metallic electrodes were integrated by the use of a combination of photopatterning and sputtering which ensures a good adhesion to the polymer surface [28]. The geometry, dimensions and shape of the electrodes can be easily tuned.

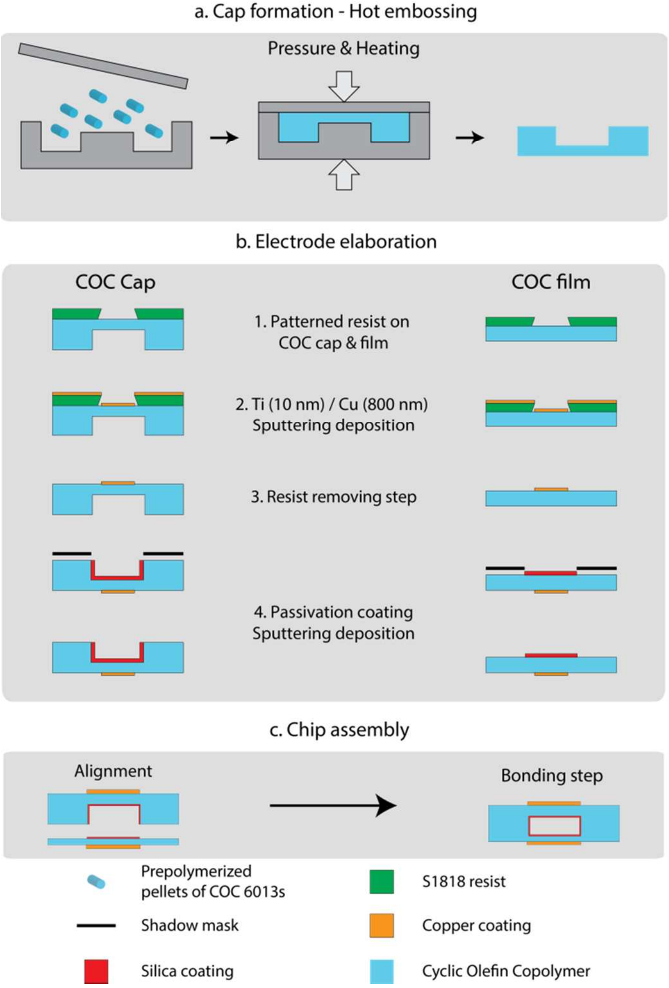

Figure 1: Principle of the multistep process investigated (a) Cap formation, (b) Electrode elaboration and (c) Chip assembly.

In addition, the inner surface of the millichannel was covered with a sputtered silica layer. This dielectric layer provides a barrier between the plasma and the polymer in order to prevent the alteration of polymer surfaces during the plasma treatment. This strategy combines advantages of both materials: the physical properties of COC including fast prototyping capability, and the well-established surface chemistry of SiO_2 thin films which could acts for further immobilization of specific molecules (metallic oxides, biomolecules …). Furthermore, previous studies have shown that the sputtered SiO_2 thin films do not affect the transparency properties of the COC film as shown in [29].

Finally, the bonding step consists in the thermal fusion bonding of the both COC parts [30].

Materials

Both COC pellets (Topas 6013S-04 Cyclic Olefin Copolymer) and thin films (Topas® 6013S, T_g = 130 °C, 254 µm thick) were purchased from Topas Advanced Polymers. S1818 photoresist and Microposit 351 Developer were obtained from Shipley®. Hexadecane ≥99% and cyclohexane ≥99% were purchased from Sigma-Aldrich (France).

Process development

The plasma chip was prepared using the following procedure:

Cleaning: COC pellets and films were first cleaned by sonication in ethanol for 30 min and then dried at 90 °C for 30 min.

Preparation of the COC cap: A few grams of the pellets were moved into an aluminum mold comprising the channel design. The molds were fabricated by micromilling (Minitech Machinery, US). The feature sizes of the straight millichannel were 50 mm length, 2 mm width and 0.5 mm depth. The mold was placed inside a heating hydraulic press (Specac) and the pellets were consequently melted at 170 °C for 10 min. A typical pressure of 2 MPa was applied for 10 min. The curing step had to be long enough in order to obtain chips without bubbles trapped inside the polymer. Finally the COC cap was released from the mold after being cooled down to room temperature.

Electrode patterning: As shown in Figure 1.b, the electrodes were elaborated by lift off on the COC cap and on a 250 µm thick COC film with the same following conditions. First, a photopatterning step was completed. A 1.8 µm thick photoresist (S1818) was spin coated on the COC substrates and cured for 90 s at 115 °C on a hotplate. Afterward, each COC substrate was aligned with a dedicated plastic mask which corresponds to the electrode geometric shapes and then UV exposed using an EVG - 620 Double Sided Mask Aligner (main exposure wavelength of 365 nm). Finally, the resist was removed from the irradiated area using a mixture of deionized water and 351 developer solution with a volume ratio of 1:4.

Electrode deposition: Sputtering was carried out using a hybrid deposition system (Plasmionique HSPT520). Once the resist layer was patterned, the electrodes were elaborated through magnetron sputtering. COC substrates were fixed on a rotated substrate holder to provide a uniform deposition. The chamber was first pumped down to reach a pressure of 5.10^{-6} Torr. Then a mixture of Ar and O_2 (2:1 mass flow ratio, Ar 20 sccm and O_2 10 sccm) was introduced into the chamber to reach the desired work pressure of 6 mTorr. First, the COC surfaces were treated by argon/oxygen plasma in order to remove the low molecular weight fragments and to favour grafting of reactive oxygenated species. This was done by applying a RF bias (13.56 MHz) on the substrate holder. Secondly, COC substrates were metallized with an 800 nm thick copper layer using DC magnetron sputtering from a 2’’ copper target 99.99% with an applied power of 100 W. Prior to copper deposition, a 10 nm thick titanium layer (2’’ Titanium target 99.97%, RF 75 W) was deposited in order to enhance the adhesion of the metallic layer onto the polymer material. The thickness of the metallic electrodes was evaluated by White Light Interferometry (Zoomsurf 3D system from Fogale Nanotech Company). The resist was finally removed in an acetone bath in combination with sonication for 30 min. The samples were consequently rinsed with ethanol and dried with N_2 stream.

Silica layer deposition: First, a shadow mask made of vacuum tape was done to localize the deposition into the inners surfaces of the channel as shown in Figure 1.b.4. The samples were consequently placed on the substrate holder to be cleaned as described for the electrode elaboration. The silica layer was deposited by RF magnetron sputtering from a 2’’ SiO_2 99.995% sputtering target with an applied power of 150 W. A mixture of Ar and O_2 was used with a mass flow ratio of 6:1 (Ar 30 sccm, O_2 5 sccm). The thickness of the deposited silica layer was measured by spectroscopic ellipsometry (HORIBA Jobin Yvon i-HR320) on a silicon substrate.

Sealing step: Before sealing the chips, the gas inlet and outlet were drilled through the COC cap. A mixture of Cyclohexane and hexadecane (3:1 volume ratio) was spread over the COC surfaces to be bonded in order to enhance the polymer chain mobility [31]. Afterwards, the upper and lower COC substrates were aligned and bonded together inside a heated hydraulic press (from Specac) at 110 °C for 3 min with an applied pressure of 0.6 MPa. Gaseous flow along the channel was ensured by plugging commercially available microfluidic connections. Figure 2 shows the final chip.

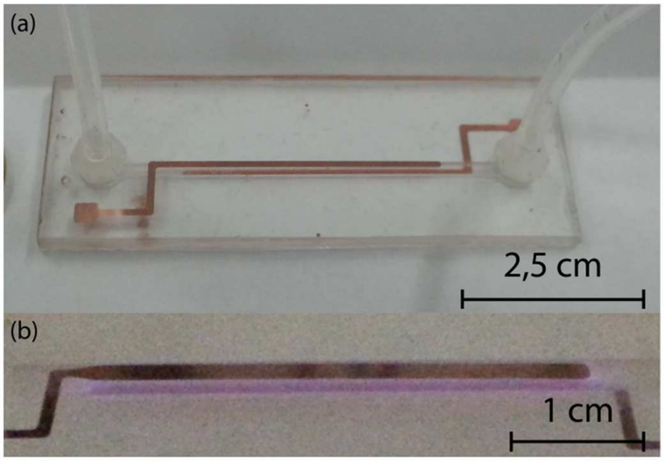

Figure 2: (a) COC plasma millireactor and (b) Air discharge performed within the millichannel. Experiment was carried out at room temperature and the plasma frequency was set at 1 kHz.

Thin film characterizations

Infrared spectra were acquired using a Fourier Transform Infrared Spectrometer (Cary 660 Spectrometer - Agilent) with an Attenuated Total Reflectance module (GladiATR - Pike).

XPS spectra were recorded using PHI 5600 XPS spectrometer (Physical Electronics, Eden Prairie, MN, USA). Survey and high resolution spectra were acquired using the Kα line of a monochromatic Al (1486.6 eV) and Mg source, respectively, operated at 150 W. Analyses were performed with a 45° angle relative to the surface. Survey spectra were acquired from 0 to 1400 eV for 15 min. Curve fitting for the high resolution peaks was completed using XPS PEAK Software (version 4.1) by means of a least square peak fitting procedure using a Gaussian-Lorentzian function and a Shirley baseline fitting. On each sample, three different spots were analysed.

Water contact angle (WCA) measurements were performed using a GBX-3S system. The advancing contact angle was measured three times on different areas of the sample and a typical deviation of ±3° with respect to the mean value was observed. The reported value corresponds to the average of these three measurements.

Experimental set-up for the VOC abatement

Experiments were performed at room temperature. The gas mixture was composed of CH_3CHO (100 ppm-mol), O_2 (20%) and N_2 (balance). The mass flow rate of the mixture to be treated was controlled by using a mass flow controller. The dielectric barrier discharge (DBD) was generated in the gaseous volume of the millichannel (Figure 2.b) (tension: 5 - 20 kV peak-to-peak voltage, frequencies: 200 Hz, sinusoidal). The power supply used to generate the sinusoidal signal was composed of a high voltage amplifier (TREK model 20/20C) and a function generator (Topward 8102 - 2 MHz). The power injected into the plasma was determined using the Manley method (V–Q Lissajous method) [17]. In this study, the injected energy is changed by varying the signal amplitude (e.g the tension), and keeping a constant signal frequency of 200 Hz. Ozone concentration in the gas outlet was evaluated using an ultra-violet absorption analyser GM-Pro (Anseros). The abatement of the acetaldehyde was assessed by GC- FID measurement (Varian 430-GC). The outlet line of the millireactor was heated in order to avoid the condensation of eventual residual acetaldehyde and water moieties which are products of the VOC oxidation.

Results and discussion

Silica layer characterizations

The measured water contact angle on the COC blank surface was equal to 90° whereas the silica coated COC films were hydrophilic with a measured water contact angle (WCA) value less than 10°. This surface wettability change was attributed to the SiO_2 film deposition. An aging study was performed by storing the silica coated samples in air for several months. The WCA values remain under a value of 20° for up to 6 months. Furthermore, in order to investigate the chemical structure of the deposited thin film, we used Fourier transform infrared spectroscopy. The spectra of the blank and the silica coated COC films are shown in Figure 3.

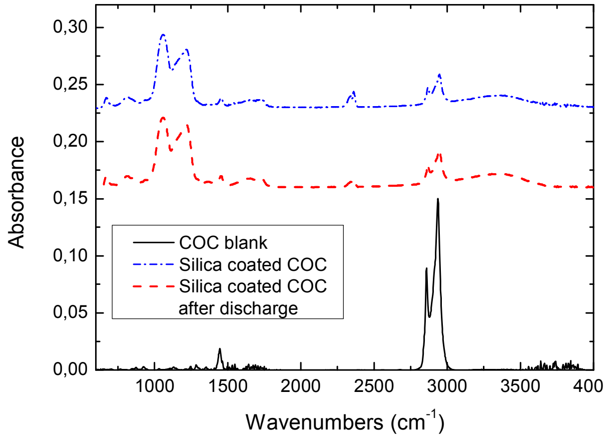

Figure 3: ATR-FTIR spectra of the (a) bare COC, (b) silica coated COC and (c) the silica coated COC after an air discharge.

In both spectra, the absorption bands located at 2947 cm^{-1} and 2868 cm^{-1} were assigned to the carbon/hydrogen stretching vibration modes of $-CH_2$ and $-CH_3$ groups from the polymer backbone. Additionally, the peak around 1454 cm-1 corresponds to the wagging mode of -CH3 groups. These peaks were significantly weaker for the silica coated sample but they were still present because of the low thickness of the silica layer of 37 ± 0.4 nm (n refractive index 1.45 at 633 nm).

The spectrum of the coated sample also shows two intense bands at 1080 cm-1 and 1200 cm-1 corresponding to the Si–O stretching modes and a vibrational band at 809 cm^{-1} associated to the Si-O bending mode. The broad absorption region around 3400 cm^{-1} was assigned to the hydroxyl group stretching mode bands. This band was related to the presence of Si–OH groups due to the interaction between the SiO_2 layer and the moisture in ambient air which leads to the formation of OH groups at the surface [32].

The surface chemical composition of the sputtered SiO_2 film was analysed by XPS measurement. The atomic compositions extracted from the survey spectra of the coated and native COC are presented in Tab. 1.

Sample	% C	% Si	% O	Si/O
Native COC	88.4	-	11.6	-
Silica coated COC	11.1	26.2	62.7	0.42

Table 1: Surface composition of COC films measured by XPS

The oxygen content of the bare COC film pointed out that the polymer surface was sensitive to oxidation when in contact with air atmosphere as already observed in [33].

Figure 4 shows the curve fitting with Si(2p) high resolution spectra of the silica coated COC samples. The Si2p high resolution spectrum was satisfactorily fitted with a single peak located at 103.9 eV and corresponding to the Si-O bonds [34]. This single peak is in good agreement with data published for sputtered silica coating and confirms the deposition of silica like film. However, the carbon content extract from the survey was also observed in the ATR-FTIR spectrum of the silica coated COC. The absorption band located between 1600 and 1750 cm^{-1} (Figure 3) was associated to the presence of carbonyl groups. This carbon content might result from the incorporation of contaminant during the deposition process. Thus, these results confirmed the presence of silica like film on the COC substrate.

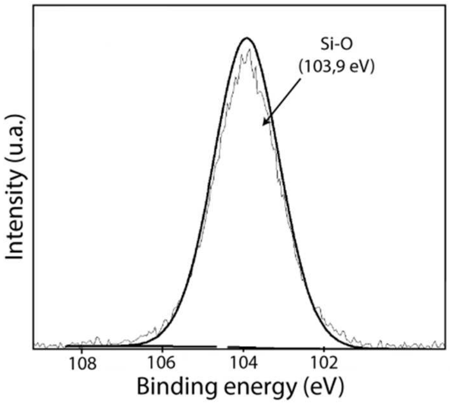

Figure 4: Si(2p) high resolution spectrum obtained by XPS measurement on silica coated COC sample.

Chemical and mechanical stability of SiO_2–COC

An air discharge (without acetaldehyde) within the millichannel was carried out for 30 min with an injected power of 0.4 W, frequency of 1 kHz and flow rate of 20 sccm of dry air. As shown in Figure 3, the comparison between the FTIR spectra prior to and after the discharge shows no significant changes in the bulk chemical bonding of the layer. This fact confirms the good stability upon etching of the protective silica layer under cold plasma conditions.

COC millireactors for VOC conversion

The emission of volatile organic compounds (VOC) is an environmental issue of major concern. Among the processes studied to efficiently remove VOC, non-thermal plasma generated in electrical discharges has many advantages. Over the last decade, many studies have been dedicated to the evaluation of the efficiency of plasma process at atmospheric pressure for the removal of VOC at low concentration (the majority being below 1000 ppm-mol) [35,36]. Indeed, the energy injected into the air plasma is dissipated through reactive process producing actives species (O, OH, O_3, NOx, N_2 vibrationally excited and metastable states, …) through reactions involving electrons, rather than heating the gas [37]. These high energy electrons and these reactive species are known to initiate removal reactions of the selected pollutant [38].

We used our plasma millireactors as a miniature source of reactive species for the purpose of VOC abatement. Figure 5 presents the acetaldehyde degradation dependence with the Specific Input Energy (SIE) which is a key parameter of atmospheric pressure plasmas. The SIE was obtained from the injected energy which was assessed by Lissajous technique and the gas flow rate using the expression presented in Eq. (1). In this study, SIE was changed by varying the high voltage (from 5 kV up to 20 kV), and keeping constant the flow rate and the frequency, and its value varies up to 325 J/L. This upper value of SIE corresponds to a maximum power injected in the plasma of 107 mW.

$$(1)\ SIE = \frac{Discharge\ power\ (W)}{Flow\ rate}$$

The gas residence time in the plasma region is 150 ms according to the gas volume of the millichannel and the injected flow rate of 20 sccm.

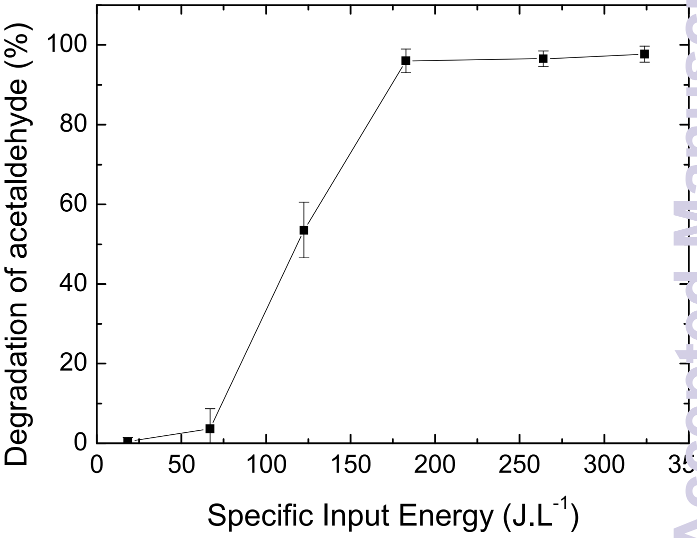

Figure 5: Acetaldehyde degradation dependence with the specific input energy. Inlet gas was composed by CH_3CHO (100 ppm), oxygen (20%) and nitrogen (balance). Experiments were carried out at room temperature and the plasma frequency was set at 200 Hz.

The residual acetaldehyde at the millireactor outlet decreased with the Specific Input Energy, and reaches 98% at 180 J/L, corresponding to a power injected into the plasma of 60 mW. When comparing these performances to recent publications [39, 40], we obtained similar results on the acetaldehyde abatement without any use of a catalytic coating inside the millichannel. This highlights the fact that the increased surface area-to-volume ratio of such millireactor leads to enhanced plasma-surface interactions. Moreover, if needed, the efficiency of our millireactors could be increased by the presence of a catalytic coating on the channel walls.

Conclusions

A simple process for manufacturing plasma millireactors was demonstrated. This process is based on the integration of metallic electrodes onto a COC chip. The inner surfaces of the millichannel were successfully covered within a silica protective layer. XPS and FTIR measurement confirmed the deposition of silica like film. The proposed plasma millireactor was used as a source of reactive species for depollution purposes. A high degradation of acetaldehyde (98 %) at room temperature was obtained for very short treatment times and specific input energy of 180 $J.L^{-1}$. Experiments are in progress to integrate catalytic coating within the millichannel for the reduction of the formation of unwanted by-products and favouring complete oxidation to CO_2 and H_2O. Moreover, such preliminary results might be very promising for using plasma millireactors as a high reactive chemical medium and bring forward new perspectives on various applications including VOC abatement, chemical synthesis such as CO_2 or CH_4 conversion in plasma millireactor.

Acknowledgements

The authors acknowledge the support of the French “Agence Nationale de la Recherche” (ANR) under the grant MicroCat and the “Institut Pierre-Gilles de Gennes” (IPGG) under the investment program Equipex ANR-10-EQPX-34. The authors wish to thank the “Conseil Général de l’Essonne” through the use of the equipment of the University Technological Center (CTU) IEF-MINERVE.

Notes and references

[a] Institut de Recherche de Chimie Paris, CNRS – Chimie ParisTech, 11 rue Pierre et Marie Curie, 75005 Paris, France.

[b] UPMC – Univ Paris 06, 4 Place Jussieu, 75005 Paris, France.

[c] Institut Curie, Centre de Recherche, UMR 168, CNRS, UPMC, F-75248 Paris.

[c] Groupe Microfluidique, MEMS et Nanostructures, Gulliver, ESPCI, 10 rue Vauquelin, 75005 Paris, France.

1 A. Grill, in *Cold Plasma in Materials Fabrication*, ed. W. Perkins, IEEE Press, Piscataway, 2nd edn., 1993, vol. 1, ch. 3, pp. 46-85.

2 A. Fridman, in *Plasma Chemistry*, Cambridge University Press, New York, 2008, ch. 4, pp. 157-258.

3 P.J. Lindner and R.S. Besser, *Chemical Engineering &Technology*, 2012, **35**, 1249.

4 A.P. Papadakis, R. Rossides and A.C. Metaxas, *The Open Applied Physics Journal*, 2011, **4**, 45.

5 H. Sekiguchi, M. Ando and H. Kojima, *Journal of Physics D: Applied Physics*, 2005, **38**, 1722.

6 D.D. Hsu and D.B. Graves, *Plasma Chemistry and Plasma Processing*, 2005, **25**, 1.

7 M.K. Kulsreshath, L. Schwaederle, L.J. Overzet, P. Lefaucheux, J. Ladroue, T. Tillocher, O. Aubry, M. Woytasik, G. Schelcher, and R. Dussart, *Journal of Physics D: Applied Physics*, **45**, 285202.

8 K. Shimizu, T. Kuwabara and M. Blajan, *Sensors*, 2012, **12**, 14525.

9 T. Seto, S.B. Kwon, M. Hirasawa and A. Yabe, *Japanese Journal of Applied Physics*, 2005, **44**, 5206.

10 T. Nozaki, A. Agiral, S. Yuzawa, J.G.E. Han Gardeniers and K. Okazaki, *Chemical Engineering Journal*, 2011, **166**, 288.

11 C. Trionfetti, A. Agiral, Han J. G. E. Gardeniers, L. Lefferts and K. Seshan, *ChemPhysChem*, 2008, **9**, 533.

12 A.C. Bose, Y. Shimizu, D. Mariotti, T. Sasaki, K. Terashima and N. Koshizaki, *Nanotechnology*, 2006, **17**, 5976.

13 F. Oshima, S. Stauss, C. Ishii, D.Z. Pai and K. Terashima, *Journal of Physics D: Applied Physics*, 2012, **45**, 402003.

14 K.H. Becker, K.H. Schoenbach and J.G. Eden, *Journal of Physics D: Applied Physics*, 2006, **39**, R55.

15 U. Kogelschatz, *Contributions to Plasma Physics*, 2007, **47**, 80.

16 H.H. Kim, A. Ogata and S. Futamura, *IEEE Transactions on Plasma Science*, 2006, **34**, 984.

17 U. Kogelschatz, *Plasma Chemistry and Plasma Processing*, 2003, **23**, 1.

18 O. Lesage, L. Falk, M. Tatoulian, D. Mantovani, and S. Ognier, *Chemical Engineering and Processing: Process Intensification*, 2013, **72**, 82-89.

19 S.K. Fan, Y.T. Shen, L.P. Tsai, C.C. Hsu, F.H. Ko and Y.T Cheng, *Lab on a Chip*, 2012, **12**, 3694.

20 P.N. Nge, C.I. Rogers and A.T. Woolley, *Chemical Reviews*, 2013, **113**, 2550.

21 Y. Ladner, F. d’Orlyé, C. Perréard, B. Da Silva, C. Guyon, M. Tatoulian, S. Griveau, F. Bedioui and A. Varenne, *Plasma Processes and Polymers,* 2014, DOI: 10.1002.

22 E. Sollier, C. Murray, P. Maoddi and D.D. Carlo, *Lab on a Chip*, 2011, **11**, 3752.

23 M. Lu, S.J. Park, B.T. Cunningham, and J.G. Edena, *Applied Physics Letters*, **92**, 2008, 101928.

24 R.K. Jena, C.Y. Yue and Y.C. Lam, *Microsystem Technologies*, 2012, **18**, 159.

25 Y. Ladner, F. d’Orlyé, C. Perréard, B. Da Silva, C. Guyon, M. Tatoulian, S. Griveau, F. Bedioui and A. Varenne, *Plasma Processes and Polymers,* 2013, **10**, 959.

26 G. Khanarian and H. Celanese, *Optical Engineering*, 2001, **40**, 1024.

27 J. Steigert, S. Haeberle, T. Brenner, C. Müller, C.P. Steinert, P. Koltay, N. Gottschlich, H. Reinecke, J. Rühe, R. Zengerle and J Ducrée, *Journal of Micromechanics And Microengineering*, 2007, **17**, 333.

28 M. Couty, M. Woytasik, J.C. Ginefri, A. Rubin, E. Martincic, M. Poirier-Quinot, L. Darrasse, F. Boumezbeur , F. Lethimonnier, M. Tatoulian and E. Dufour-Gergam, *Polymers*, 2012, **4**, 656.

29 K.S. Ma, F. Reza, I. Saaem and J. Tian, *Journal of Materials Chemistry*, 2009, **19**, 7914.

30 C.W. Tsao and D.L. DeVoe, *Microfluid Nanofluid*, 2009, **6**, 1.

31 S. Miserere, G. Mottet, V. Taniga, S. Descroix, J.L. Viovy and L. Malaquin, *Lab on a Chip*, 2012, **12**, 1849.

32 C.C. Perry and X.C. Li, *Journal of the Chemical Society*, 1991, **87**, 761.

33 S. Roy, C.Y. Yue, Y.C. Lam, Z.Y. Wang and H. Hu, *Sensors and Actuators B: Chemical*, 2010, **150**, 537.

34 M.R. Alexander, R.D. Short, F.R. Jones, W. Michaeli and C.J. Blomfield, *Applied Surface Science*, 1999,**137**, 179.

35 A.M. Vandenbroucke, R. Morent, N. De Geyter and C. Leys, *Journal of Hazardous Materials*, 2011, **195**, 30.

36 H.H. Kim, *Plasma Processes and Polymers*, 2004, **1**, 91.

37 J.Van Durme, J. Dewulf, C. Leys, H. Van Langenhove*, Applied Catalysis B: Environmental*, 2008, **78**, 324.

38 H.L. Chen, H.M. Lee, S.H. Chen, M.B. Chang, S.J. Yu and S.N. Li, Environmental Science & Technoly, 2009, **43**, 2216.

39 C. Klett, S. Touchard, A. Vega-Gonzalez, M. Redolfi, X. Bonnin, K. Hassouni and X. Duten, *Plasma Sources Science and Technology*, 2012, **21**, 045001.

40 Z. Jia, A. Vega-Gonzalez, M.B. Amar, K. Hassouni, S. Tieng, S. Touchard, A. Kanaev, and X. Duten, *Catalysis Today*, 2013, **208**, 82.